Atomic-scale studies of cobalt distribution in Co–TiO_2 anatase thin films: Processing, microstructure, and the origin of ferromagnetism

K. A. Griffin
Department of Materials Science and Engineering, University of Washington, Seattle, Washington 98195

M. Varela and S. J. Pennycook
Condensed Matter Sciences Division, Oak Ridge National Laboratory, Oak Ridge, Tennessee 37831

A. B. Pakhomov and Kannan M. Krishnan[a)]
Department of Materials Science and Engineering, University of Washington, Seattle, Washington 98195

(Presented on 2 November 2005; published online 21 April 2006)

Using high-resolution, aberration-corrected, scanning transmission electron microscopy and electron-energy-loss spectroscopy we show that in films of single-phase anatase Co:TiO_2, the Co distribution and magnetic properties are strongly dependent both on the overall crystalline quality and postgrowth vacuum annealing process. The Co:TiO_2 films are coherent, epitaxial anatase with no secondary phases or metallic Co. Films of lower crystalline quality reveal a relatively homogeneous Co concentration, while films of higher crystalline quality show a tendency for Co enrichment near the surface region, around grain boundaries, and the substrate interface. Both uniform and nonuniform samples show a notable enhancement in the saturation magnetization with annealing, while the coercive field is considerably higher in the samples with uniform Co distribution. These experiments confirm that films of single-phase anatase Co:TiO_2 with both uniform and nonuniform Co distributions exhibit room-temperature ferromagnetism in the insulating ground state, while the compositional uniformity and film microstructure play a role in the bulk magnetic properties of the material and the mechanisms for ferromagnetic ordering.
 [DOI: 10.1063/1.2170068]

The technological promises of spintronics[1–3] have led to a push in research of materials suitable for room-temperature (RT) device applications. Even though transition-metal-doped oxides have emerged as possible dilute magnetic semiconductor (DMS) materials for spintronics,[4–8] many questions remain regarding the origin of their ferromagnetism (FM) and its correlation to semiconducting properties. With the discovery of RTFM in Co-doped anatase TiO_2,[4] this material has been at the forefront of material research for a RT DMS, and reports on both Co- and Cr-doped anatase TiO_2 thin films have shown that they can be both highly insulating and FM at room temperature,[9–11] in conflict with the model of carrier-mediated-type exchange exhibited by Mn:GaAs.[3] These results show that transition-metal-doped oxides such as Co:TiO_2 may, in fact, be referred to as dilute magnetic dielectrics,[9,12] and their ferromagnetism may have alternative explainations.[13] Previously, high magnetic moments in anatase Co:TiO_2 have been attributed to the presence of nanoscale regions of highly Co-enriched anatase;[7,14] however, we have recently reported strong FM even in films with uniform Co distribution in the anatase lattice.[9] In this paper we confirm that we can synthesize films of anatase TiO_2 with a homogeneous Co distribution that are intrinsically FM at RT, and with suitable processing conditions, we can control the Co distribution to be uniform or nonuniform. Both uniform and nonuniform films exhibit RTFM without the presence of secondary phases, while the bulk magnetic properties can be directly correlated to differences in compositional uniformity and film microstructure. The detailed chemical analysis and magnetic measurements suggest that in uniform and nonuniform Co-distributed anatase films, the origins of FM may be from differing mechanisms.

The details of the growth of our Co-doped anatase TiO_2 thin films by rf magnetron sputter deposition are described in previous work.[9] Here, we investigate films with 3.5 at. % Co grown on $LaAlO_3$ (100) (LAO) substrates of two different qualities: films grown on a higher-quality substrate (LAO with a physical surface roughness of <2 Å) to be called "sample A," and those grown on a lower-quality substrate (LAO with a roughness of <5 Å), which are identical to those discussed previously,[9] to be called "sample B." After growth, all films were also vacuum annealed at $<10^{-5}$ Torr for 1 h at 450 °C. X-ray-diffraction (XRD) techniques were used for analyzing the crystal structure/quality of the samples. We have performed a detailed atomic to micron scale study using high-resolution, aberration-corrected, scanning transmission electron microscopy (STEM) and electron-energy-loss spectroscopy (EELS) to map the Co distribution as a function of annealing and crystalline quality. Comparative studies on a superconducting quantum interference device magnetometer showed corresponding differences in magnetic properties.

From high-angle XRD all films were found to be single-phase anatase (004) oriented on the closely lattice-matched LAO substrates with no evidence of secondary phases. The full width at half maximum (FWHM) in 2-theta ($2\theta_{FWHM}$) of the anatase (004) peak was used to calculate the grain size from the Scherrer equation:[15] 120 Å for sample A and 100 Å

[a)]Author to whom correspondence should be addressed; electronic mail: kannanmk@u.washington.edu

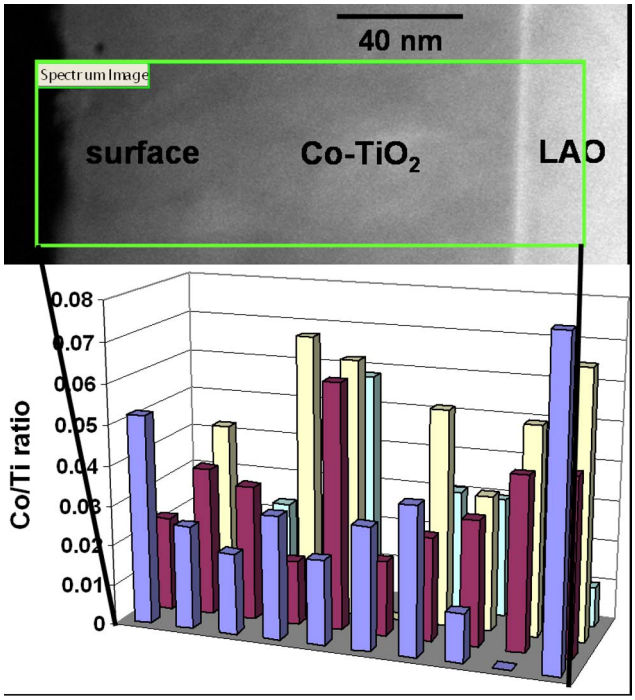

FIG. 1. (Color online) HAADF image of a surface region of the annealed sample B Co–TiO_2 film, with an inset of the three-dimensional Co/Ti ratio map calculated from the EELS core-loss spectrum image.

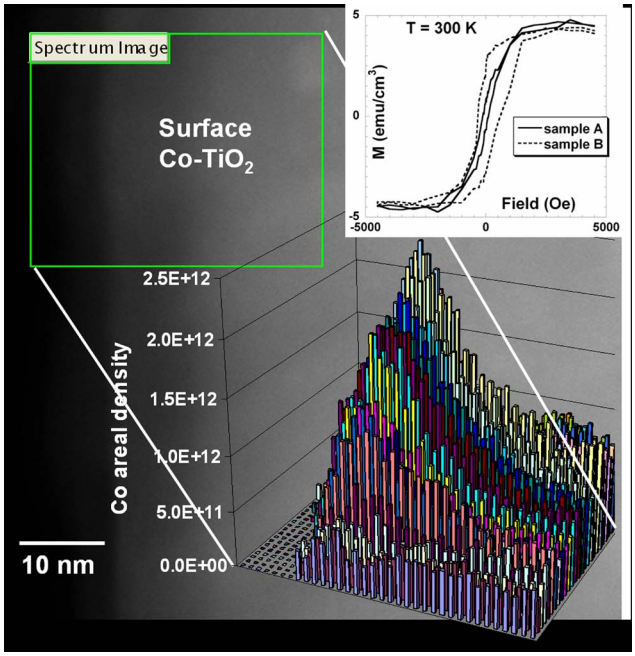

FIG. 2. (Color online) HAADF image of the annealed sample A Co–TiO_2 film, with an inset of the cobalt areal density map calculated from the EELS low-loss spectrum image. The Co *M* edge areal density has been normalized by the film thickness. Inset: *M-H* loops at 300 K of annealed sample A (solid line) and annealed sample B (dashed line) Co:TiO_2 films. (The diamagnetic contribution from the LAO substrate has been subtracted from the experimental data.)

for sample B. With annealing, the crystal size increased to 165 and 125 Å, respectively. The measurements of the FWHM in theta (θ_{FWHM}) from the XRD rocking curve scan indicated a well-oriented (004) anatase structure in both samples, with little to no change after annealing.

The STEM and EELS results were obtained at the ORNL using the VG Microscope HB501UX operated at 100 kV with a Nion aberration corrector. The high resolution of the 501 gives a beam size of 1 Å and an energy resolution of 0.5 eV, where the EELS can be performed with atomic resolution, limited only by the size of the probe.[16,17] Low-loss (LL) EELS spectrum images (SIs) were used to map the Co distribution in the film by using a 10 eV window at the Co $M_{2,3}$ edge at 60 eV. A Hartree-Slater cross section was used for the Co $M_{2,3}$ edge analysis, and the Co areal density map was normalized by a thickness map calculated from the zero-loss peak. Core-loss (CL) SIs were also taken on a number of locations throughout the samples. With the core-loss spectra the Co, Ti, and O areal densities and the Co/Ti ratios were calculated from the Co and Ti *L* edges (at 779 and 456 eV, respectively, using hydrogenic cross sections including corrections for white lines) and the O *K* edge (at 532 eV, using a Hartree-Slater cross section). All films (samples A and B, as-deposited and annealed) were single-phase anatase TiO_2 with Co dissolved in the lattice. This was determined from high-resolution imaging and analysis of the energy-loss near-edge structure (ELNES) of the Co ions.[18]

As-deposited Co–TiO_2 *films*. A number of EELS SIs taken at a range of magnifications confirmed that the Co distribution is homogeneous within ±3 at. % throughout all the areas of the as-deposited sample B. From LL SIs, regions near the surface and substrate show a slight increase (~1.2 × bulk content) in Co but there were no truly Co-rich regions. The Co distribution in the as-deposited sample A was strikingly different from sample B. The CL and LL maps show Co-enriched anatase regions near the surface with up to 4× that of the bulk (corresponding to 12 at. % Co), and some evidence for enrichment in close proximity to grain-boundary regions and the substrate interface. However, it is worth noting that the Co-enriched surface regions of sample A are within the top 20 nm of the 95 nm anatase film thickness, there are no surface islands of Co-enriched anatase, and no evidence of secondary phases.

Annealed Co–TiO_2 *films*: Sample B showed no significant change in Co distribution with annealing. The results from the LL maps indicate a slight increase in Co content near the surface and substrate interface of up to 1.5× that of the bulk. The CL maps give a mean Co/Ti value of 0.03±0.03 across the entire film thickness and up to 0.07 near the substrate interface. Figure 1 demonstrates a high angle annular dark field (HAADF) image of the annealed sample B, where the CL SIs were taken from the boxed area, and the corresponding calculated Co/Ti ratios are plotted in three dimensions. The effect of annealing in sample A, however, was easily noticeable and markedly different from sample B, as seen by the LL and CL maps. The LL maps reveal a strong Co enrichment near the surface, up to 7× the bulk. On average, the Co content tends to be higher in the top 20 nm of the film (averaging about 3–7 at. % Co) and lower in the bulk (less than 1 at. % Co), similar to as-deposited sample A. This Co enrichment in the 20 nm top surface layer can easily be seen in the LL Co areal density map of a region near the film surface shown in Fig. 2. Again, the mapping also showed some enrichment near the substrate

interface and grain-boundary regions. It is important to note again that from the high-resolution imaging and ELNES analysis, these Co- rich regions were all still coherent anatase, with no secondary phases.

Magnetic hysteresis loops (M vs H) at 300 K show that the as-deposited sample B (uniform) is weakly FM with a saturation magnetization, M_S, of $0.15\mu_B$/Co atom and a coercivity, H_C, of 100 Oe, while the films are highly insulating. With annealing magnetic properties are significantly enhanced with an increase in M_S to $\sim 0.65\mu_B$/Co atom, H_C to 350 Oe, and remanence (M_R/M_S) to 0.60 (inset of Fig. 2), while the sample remains highly insulating with the resistivity at least $>10^6\ \Omega$ cm. Meanwhile, the as-deposited sample A (nonuniform) does not exibit RTFM, but under the same annealing conditions, becomes FM with $M_S \sim 0.7\mu_B$/Co atom, $H_C \sim 150$ Oe, and $M_R/M_S \sim 0.17$ (inset of Fig. 2), and remains highly insulating.

The experimental results reveal a number of interesting points. First, the evidence of RTFM in both uniform and nonuniform annealed films of single-phase anatase $Co:TiO_2$ proves that a FM insulating ground state can exist for different levels of magnetic dopant uniformity. In addition, the annealing process is required for activation of FM in both uniform and nonuniformly doped films. In the case of uniform Co distribution (B), the activation of FM is most likely related to the creation and diffusion of oxygen vacancies (V_O's).[9] For films with a nonuniform Co distribution (A), the activation correlates with both the migration of Co ions and possible creation/diffusion of V_O's in the anatase lattice. Another key observation is the absence of RTFM in the as-deposited sample A (with some anatase regions ~ 12 at. % Co), where we see that the formation of Co-enriched anatase regions alone does not provide the necessary conditions for RTFM. Most interestingly, we notice that while the M_S values of annealed samples A and B are relatively close in value, the films with a homogeneous Co distribution (B) have considerably higher coercivities and remanence. We attribute the latter to the different magnetization reversal processes due to microstructural defects and local variations in composition. The increased number of structural defects (grain boundaries and stacking faults) in sample B may also act as nucleation sites for Co-V_O defect formation during the postgrowth annealing.[19] One must also consider the effects of differing levels of Co uniformity on the possible mechanisms for FM ordering in the films. In highly Co-enriched regions, which can exist locally in inhomogeneous samples (see Ref. 7 and sample A in the present work), the average distance between Co ions is relatively small (approximately few angstroms). Meanwhile, in homogeneous solutions (Refs. 9 and 12 and sample B in this work) with a random Co dopant distribution, the probability of finding Co ions with Co next-nearest neighbors would be lower ($\sim 30\%$). We see that both cases result in FM and insulating films, demonstrating that either the mechanism for FM ordering is correlated with Co–Co distances and is different in uniform versus nonuniformly doped films, or if the mechanism is the same, then the FM ground state does not require a majority of Co dopants to be situated in Co–O–Co configurations. Although the experimental evidence of the activation of RTFM in both uniform and nonuniformly doped films leaves us with many questions regarding the origin of FM, the main result of our experiment is that anatase $Co:TiO_2$ films with both inhomogeneous and homogeneous Co distributions can exhibit RTFM in the insulating ground state, where the bulk magnetic properties are affected by the film microstructure and compositional uniformity.

The detailed EELS compositional analysis of single-phase anatase $Co:TiO_2$ has shown that there is a strong correlation between the processing and microstructure of the films to the Co distribution and the bulk magnetic properties. Results demonstrate that films with both uniform and nonuniform Co distributions exhibit room-temperature ferromagnetism in the insulating ground state, which is activated by a postgrowth vacuum annealing process. The microstructure and magnetic dopant uniformity strongly influence the bulk magnetic properties, magnetization reversal processes, and mechanism for magnetic ordering.

The authors thank S. Chambers for helpful discussions and B. Sides and J. Luck for experimental assistance. The work at the UW was funded by NSF/ECS Grant No. 0224138 and the Campbell Endowment, with partial support to one of the authors (K.A.G.) received from UW-PNNL JIN (2005) fellowship. Research at ORNL is sponsored by the Laboratory Directed Research and Development Program of ORNL, managed by UT-Batelle, LLC, for the U.S. Department of Energy under Contract No. DE-AC05-00OR22725.

[1] S. A. Wolf *et al.*, Science **294**, 1488 (2001).
[2] H. Ohno, Science **281**, 951 (1998).
[3] T. Dietl, H. Ohno, F. Matsukura, J. Cibert, and D. Ferrand, Science **287**, 1019 (2000).
[4] Y. Matsumoto *et al.*, Science **291**, 854 (2001).
[5] S. J. Pearton *et al.*, J. Appl. Phys. **93**, 1 (2003).
[6] T. Fukumura, Z. Jin, A. Ohtomo, H. Koinuma, and M. Kawasaki, Appl. Phys. Lett. **75**, 3366 (1999).
[7] S. A. Chambers *et al.*, Appl. Phys. Lett. **79**, 3467 (2001).
[8] T. Dietl, Nat. Mater. **2**, 646 (2003).
[9] K. A. Griffin, A. B. Pakhomov, C. M. Wang, S. M. Heald, and K. M. Krishnan, Phys. Rev. Lett. **94**, 157204 (2005).
[10] T. Droubay *et al.*, J. Appl. Phys. **97**, 046103 (2005).
[11] T. Zhao *et al.*, Phys. Rev. Lett. **94**, 126601 (2005).
[12] K. A. Griffin *et al.*, J. Appl. Phys. **97**, 10D320 (2005).
[13] J. M. D. Coey, A. P. Douvalis, C. B. Fitzgerald, and M. Venkatesan, Appl. Phys. Lett. **84**, 1332 (2004); J. M. D. Coey, M. Venkatesan, and C. B. Fitzgerald, Nat. Mater. **4**, 173 (2005).
[14] S. A. Chambers *et al.*, Appl. Phys. Lett. **82**, 1257 (2003).
[15] B. E. Warren, *X-ray Diffraction* (Dover, New York, 1990).
[16] *Z*-contrast images were obtained by collecting, point by point, the Rutherford-scattered electrons at high angles using an annular dark-field (HAADF) detector. Energy-loss electrons passing through the central hole in the detector were collected simultaneously with the HAADF image.
[17] M. Varela *et al.*, Phys. Rev. Lett. **92**, 095502 (2004); N. D. Browning, M. F. Chisholm, and S. J. Pennycook, Nature (London) **366**, 143 (1993); G. Duscher, N. D. Browning, and S. J. Pennycook, Phys. Status Solidi A **166**, 327 (1998); U. Kaiser *et al.*, Nat. Mater. **1**, 102 (2002); B. Rafferty and S. J. Pennycook, Ultramicroscopy **78**, 141 (1999); L. J. Allen *et al.*, Phys. Rev. Lett. **91**, 105503 (2003).
[18] K. A. Griffin, M. Varela, S. J. Pennycook, and K. M. Krishnan, unpublished ELNES data.
[19] The correlation of interfacial defects to FM activation has previously been demonstrated in transition-metal-doped oxide nanocrystals, see P. V. Radovanovic and D. R. Gamelin, Phys. Rev. Lett. **91**, 157202 (2003); J. D. Bryan, S. M. Heald, S. A. Chambers, and D. R. Gamelin, J. Am. Chem. Soc. **126**, 11640 (2004).